IOSR Journal of Mechanical and Civil Engineering (IOSR-JMCE)
e-ISSN: 2278-1684,p-ISSN: 2320-334X, Volume 13, Issue 5 Ver. III (Sep. - Oct. 2016), PP 93-98
www.iosrjournals.org

Effect of Yttrium Oxide Doping on CTE of Al/ZrO_2 Metal Matrix Composites

A. Chennakesava Reddy
Professor, Department of Mechanical Engineering, JNTUH College of Engineering, Hyderabad

Abstract: *Aluminum-zirconia based metal matrix composites reinforced with zirconia nanoparticles were prepared by powder metallurgy route. The zirconia nanoparticles were doped with yttria. The thermal expansion behaviors of the metal matrix composites with various zirconia contents (5.0; 10.0; 15.0; 20.0; 25.0 vol.%) and doping with 8% and 15% yttria were investigated. Results indicated that increasing the yttria doping content improved the stability of zirconia crystallographic phase and avoided tetragonal to monoclinic transformation. The results revealed that the nanoparticle volume fraction had significant effect on the thermal expansion behavior of the composites. The thermal expansion of the composites was within the Turner's, Kerner's and Schapery's models.*

Keywords: *Metal matrix composites, coefficient of thermal expansion, zirconia, yttria.*

I. Introduction

Aluminum metal matrix composites have been studied to improve the physical and mechanical properties for more than half a century. The physical and mechanical properties are radically influenced by the volume fraction, distribution, size and shape parameters of the reinforced particles [1]. Among these various factors, the volume fraction of the ceramic particles is the most important. Several reinforcement particles such as Al_2O_3 [2], SiC [3], SiO_2 [4], Si_3N_4 [5], B_4C [6], TiC [7], TiN [8], ZrC [9], MgO [10], and BN [11] are being used to prepare aluminum metal matrix composites. The thermal stability makes them a good choice for use as reinforcing materials in aerospace and transport industries. Even though the mechanical behavior of composites is known significantly over the two decades, the crystallographic transformation of the reinforced particles still remains challenging [12]. Due to the different thermal expansion coefficients of matrix and reinforcement, internal stresses are developed at the interface between the metal-matrix and the ceramic phase during processing of the composite or during thermal cycling [13]. By varying the matrix, reinforcement and volume fractions, the metal matrix composites can be customized to provide a good coefficient of thermal expansion (CTE) matching for thermal management and thermal conductivity. It is necessary to evaluate new materials for their thermal stability and to measure their properties including CTE for products, such as break discs made from castings, before actual use.

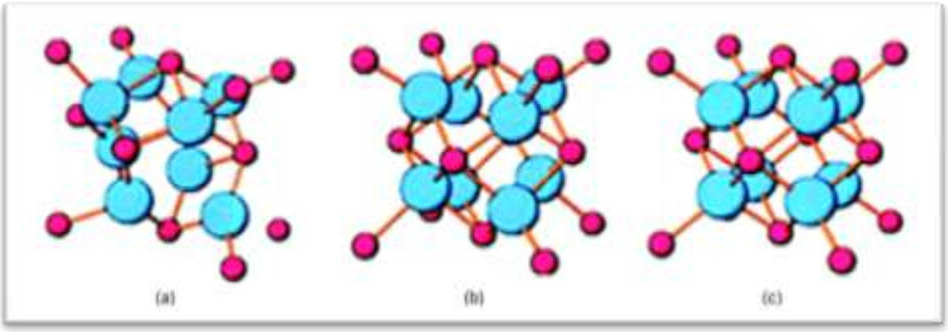

Figure 1: Three crystalline forms of zirconia: (a) monoclinic, (b) tetragonal and (c) cubic.

Zirconium dioxide (ZrO_2), also known as zirconia is a white crystalline oxide of zirconium. Zirconia has three crystalline forms as illustrated in figure 1. ZrO_2 has monoclinic crystal structure at room temperature and undergoes transformations to tetragonal and cubic at higher temperatures. The stability of three crystalline forms is as follows: monoclinic <1170 °C, tetragonal 1170–2370 °C, and cubic >2370 °C. The volume expansion caused by the cubic to tetragonal to monoclinic transformation induces large stresses, and these stresses cause ZrO_2 to crack upon cooling from high temperatures [14]. When the zirconia is blended with some other oxides, the tetragonal and/or cubic phases are stabilized. Effective dopants include MgO, Y_2O_3, CaO, and Ce_2O_3 [15]. Some thermal-expansion curves for Al/ZrO_2 composites had been published, but these did not contain information upon which an explanation for the structural weakening could be based.

The present study emphases on determining the effective linear thermal expansion coefficient (CTE) of Al/ZrO_2 metal matrix composites with and without addition of yttrium oxide (Y_2O_3). The theoretically predicted CTE values have been compared with the experimental values.

II. Materials and Methods

Pure Al powder of 100 µm with 99.9% purity and ZrO_2 powders of 100 nm without and with doping by Y_2O_3 were used as the starting materials. Pure powders of Al and ZrO_2 (both doped and non-doped), in the desired volume fractions, were mixed together by high-energy ball milling for 20 h to ensure the uniform mixing. The non-doped and doped zirconia powders are shown in figure 2. The mixing was carried out in argon atmosphere to minimize the contamination. The obtained powder mixtures were then sintered to bulk specimens (figure 3) by hot pressing at 800°C with a pressure of 50 MPa in vacuum, followed by quickly cooling to room temperature in 30 min. In this study, four different composites were prepared (Table 1).

Table 1: Composition of metal matrix composites

Composite	Composition, vol.%		Doping, %
	Al	ZrO_2	Y_2O_3
AL-ZRO-1	95	5.0	-
AL-ZRO-2	90	10.0	-
AL-ZRO-3	85	15.0	-
AL-ZRO-4	80	20.0	-
AL-ZRO-5	75	25.0	-
AL-ZRO-YO-6	95	5.0	8.0
AL-ZRO-YO-7	90	10.0	8.0
AL-ZRO-YO-8	85	15.0	8.0
AL-ZRO-YO-9	80	20.0	8.0
AL-ZRO-YO-10	75	25.0	8.0
AL-ZRO-YO-11	95	5.0	15.0
AL-ZRO-YO-12	90	10.0	15.0
AL-ZRO-YO-13	85	15.0	15.0
AL-ZRO-YO-14	80	20.0	15.0
AL-ZRO-YO-15	75	25.0	15.0

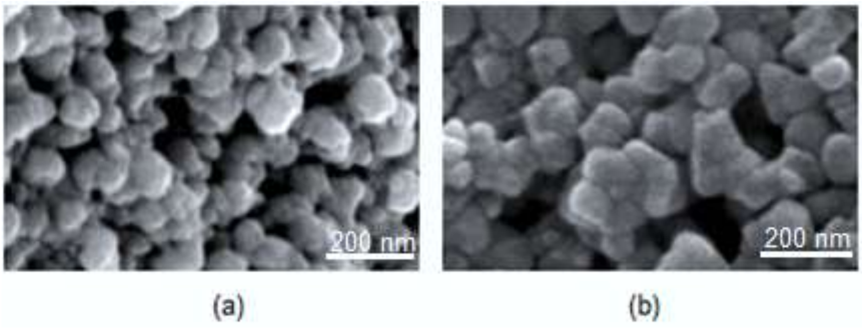

Figure 2: Pure zirconia (a) and doped zirconia with 15% yttria (b).

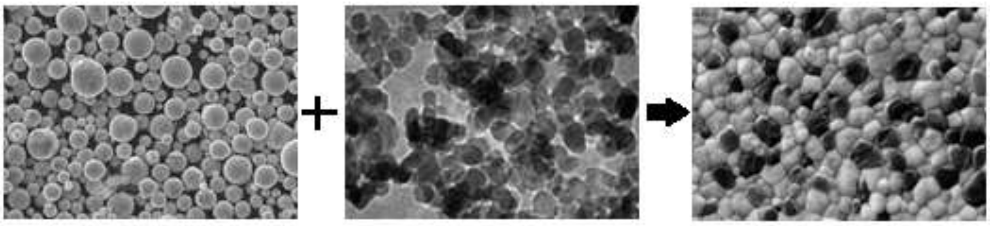

Figure 3: Preparation of Al/ZrO_2 metal matrix composites by powder metallurgy route.

The thermal expansion was then measured with a dilatometer (DIL 802) between 100 and 300°C at heating and cooling rates of 5°C/min in argon. With this instrument the difference in length between the specimen to be investigated and a reference sample is measured, which results in a resolution of ± 0.01 µm. Specimens with a diameter of 5 mm and length of 10 mm were used to measure CTE. The instantaneous CTE at a given temperature was calculated using the following equation:

$$\mathrm{CTE} = \frac{\partial}{\partial T}\left(\frac{\Delta L}{L}\right) \quad (1)$$

where L is the length of the specimen and T the temperature. All of the specimens were tested from 30°C to 400°C for heating cycle and 400°C to 30°C during cooling cycle at 10°C/min. This temperature range was selected so as to include the entire usable range of the Al/ZrO_2 metal matrix composites, without the formation of liquid phase in the matrix.

III. Results and Discussion

All powder materials consist of agglomerates of submicron size. The degree of agglomeration is similar for all prepared compositions independent on ZrO_2 content. The microstructures of composites reinforced with pure ZrO_2 nanoparticles and ZrO_2 nanoparticles doped by Y_2O_3 are shown in optical microscopy images (figure 4). The distribution of ZrO_2 nanoparticles is random with no cracks and deleterious pores in the microstructure. The measured microscopic porosities were found between 1.5 % – 2.5 % for produced metal matrix composites.

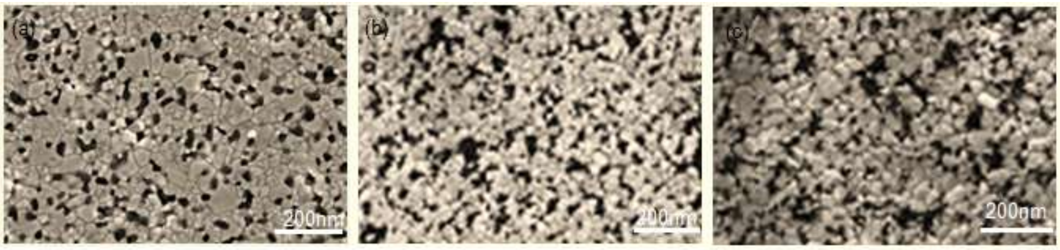

Figure 4: Microstructures of Al/ZrO_2 composites: (a) 30 vol.% pure ZrO_2 (b) 30 vol.% ZrO_2 doped with 8% Y_2O_3 and (c) 30 vol.% ZrO_2 doped with 15% Y_2O_3.

3.1 Coefficient of thermal expansion

The relative thermal expansion behavior of aluminum zirconia based metal matrix composites reinforced with non-doped and doped ZrO_2 nanoparticles measured at temperatures varying from 30°C to 400°C for a single thermal cycle are shown in figure 3. The CTE measured during the heating cycle increases with increasing temperature between 30 and 400°C for all the composites. There is evident variation in heating and cooling curves. The CTE measured during the cooling cycle decreases continuously with decreasing temperature in the same trend but above of the heating cycle. The difference in CTE during heating and cooling is due to difference in CTE of Al matrix and ZrO_2 nanoparticles. In a two-phase system composed of a continuous Al matrix and non-doped ZrO_2 nanoparticles, the gap between the CTE curves due to change of volume fraction of ZrO_2 is wide of nearly $1.62\text{x}10^{-6}$/°C. This gap is reduced in a three phase system as shown in figure 3b and 3c. This gap is diminished due to increased doped content of Y_2O_3. So the thermal expansion behavior of the composite is the result of the interaction between Al matrix and ZrO_2 nanoparticles through the doped Y_2O_3 interfaces. Upon heating, zirconia undergoes disruptive phase changes. By adding small percentages of yttria, these phase changes are eliminated.

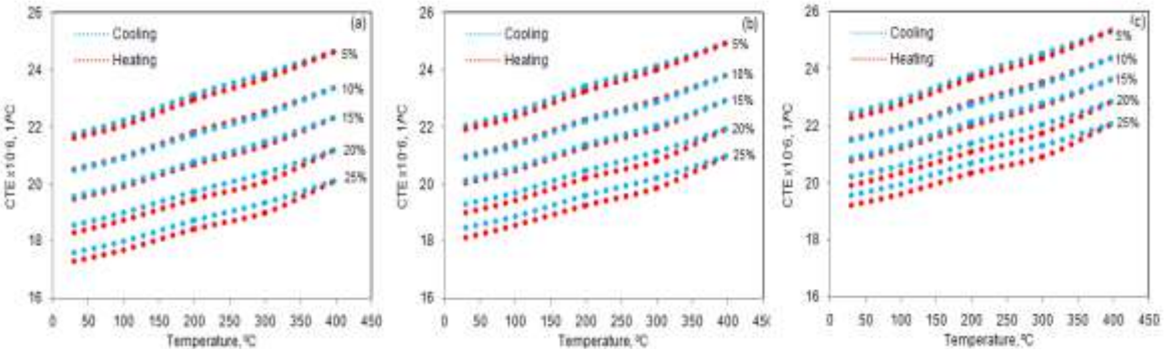

Figure 3: Coefficient of thermal expansion as a function of temperature for: (a) 100% ZrO_2, (b) 85% ZrO_2 doped with 10% Y_2O_3 and (c) 85% ZrO_2 doped with15% Y_2O_3.

3.2 Comparison of CTEs among experimental and theoretical results

In order to understand the thermal expansion behavior of the composites well, it is imperative to relate quantitatively theoretical predictions with experimental results. Many analytical and semi-empirical formulas have been derived to evaluate the effective coefficient of the linear thermal expansion of different types of heterogeneous composites [16-18]. The rule-of-mixture models are derived from the assumption of uniform strain or stress of the composite structure.

$$\alpha_c = \alpha_r V_r + \alpha_m V_m \qquad (2)$$

Turner model [16] takes into account the mechanical interaction between the phases in the heterogeneous composite material.

$$\alpha_c = \frac{\alpha_m V_m K_m + \alpha_r V_r K_r}{V_m K_m + V_r K_r} \tag{3}$$

Another model for particulate composites is given by Kerner [17], which accounts for both shear and isostatic stresses developed in the component phases, and gives the CTE for the composite as:

$$\alpha_c = \alpha_m V_m + \alpha_r V_r + V_m V_r (\alpha_r - \alpha_m) \frac{K_r - K_m}{V_m K_m + V_r K_r + 3K_m K_r / 4G_m} \tag{4}$$

Schapery [18] used elastic energy principles to derive bounds for effective CTEs of anisotropic composites made from isotropic constituents. The lower and upper bounds for the effective coefficients are given by

$$\alpha_c^u = \alpha_m V_m + \alpha_r V_r + \frac{4G_m}{K_c} \frac{(K_c - K_r)(\alpha_m - \alpha_r) V_r}{4G_m + 3K_r} \tag{5}$$

$$\alpha_c^l = \alpha_m V_m + \alpha_r V_r + \frac{4G_r}{K_c} \frac{(K_c - K_m)(\alpha_r - \alpha_m) V_m}{4G_m + 3K_m} \tag{6}$$

where α is the CTE, v is the volume fraction, K is the bulk modulus, G is the shear modulus, and subscripts c, m, r refer to the composite, matrix and particle respectively.

Figures 4 to 8 compare the experimental results with the theoretical models for all fifteen metal matrix composites. In all the cases, the upper bound of composite CTE is Schapery's upper bound and the lower bound of composite CTE is Schapery's lower bound. The experimental CTEs for entire temperature range show significantly deviation from Turner's model. This is owing to Turner's model is based on the fact that only uniform hydrostatic stresses exist in the phases, while the stresses inside the composite are very complex. Kerner's model, which assumes spherical particles, may underestimate the actual constraints in the composite. Even though the range of operating temperature is 0 to 400°C, the CTE curves are slightly non-linear in the composites having non-doped ZrO$_2$ nanoparticles. This is owing to metastable tetragonal phase of ZrO$_2$. If sufficient quantities of the metastable tetragonal phase are present, then an applied stress, magnified by the stress concentration at a crack tip, can cause the tetragonal phase to convert to monoclinic, with the associated volume expansion. This phase transformation can then put the crack into compression, retarding its growth, and enhancing the fracture toughness. This mechanism is known as transformation toughening. With doping of ZrO$_2$ nanoparticles with Y$_2$O$_3$, the transformation toughening is eliminated.

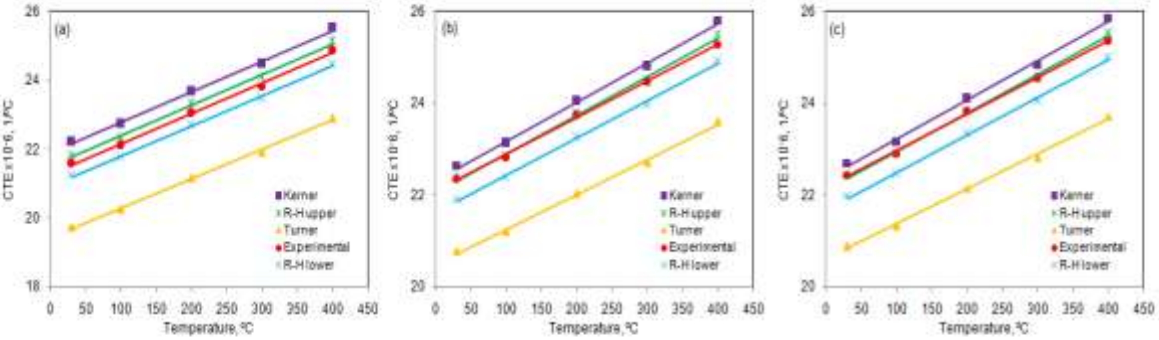

Figure 4: Coefficient of thermal expansion as a function of temperature for AA1100/5%vf: (a) 100% ZrO$_2$, (b) 85% ZrO$_2$ doped with 8% Y$_2$O$_3$ and (c) 85% ZrO$_2$ doped with15% Y$_2$O$_3$.

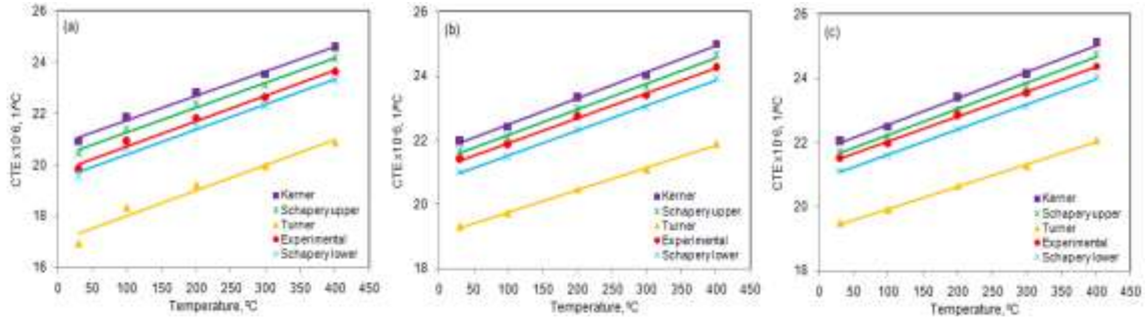

Figure 5: Coefficient of thermal expansion as a function of temperature for AA1100/10%vf: (a) 100% ZrO$_2$, (b) 85% ZrO$_2$ doped with 8% Y$_2$O$_3$ and (c) 85% ZrO$_2$ doped with15% Y$_2$O$_3$.

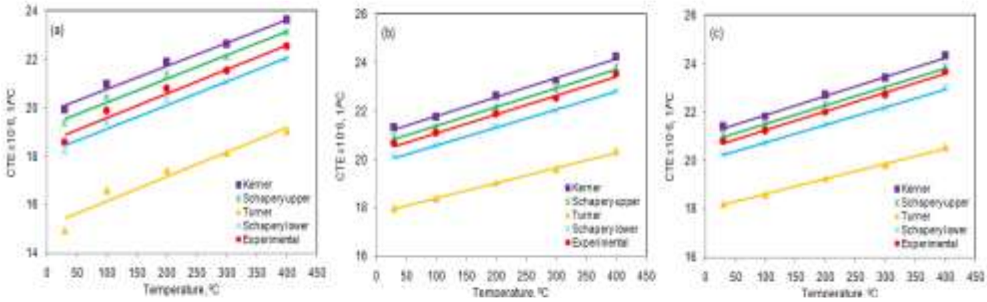

Figure 6: Coefficient of thermal expansion as a function of temperature for AA1100/15%vf: (a) 100% ZrO_2, (b) 85% ZrO_2 doped with 8% Y_2O_3 and (c) 85% ZrO_2 doped with15% Y_2O_3

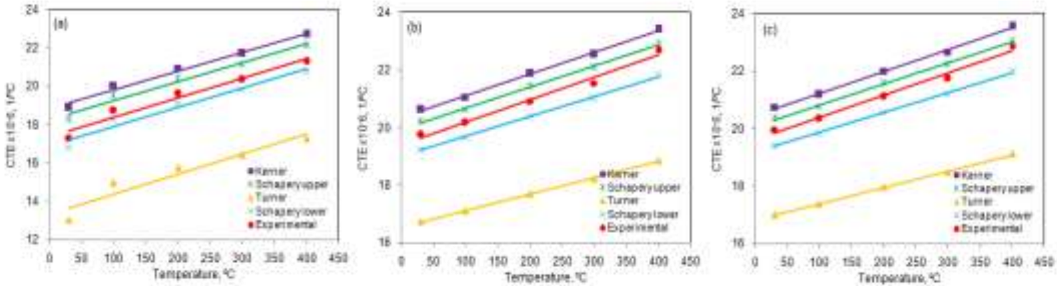

Figure 7: Coefficient of thermal expansion as a function of temperature for AA1100/20%vf: (a) 100% ZrO_2, (b) 85% ZrO_2 doped with 8% Y_2O_3 and (c) 85% ZrO_2 doped with15% Y_2O_3.

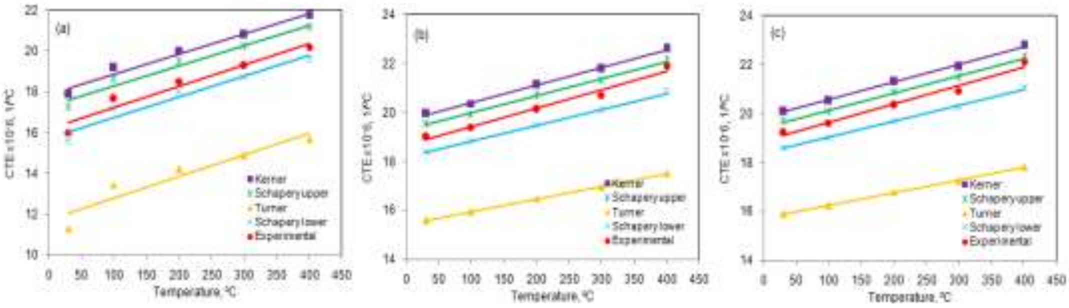

Figure 8: Coefficient of thermal expansion as a function of temperature for AA1100/25%vf: (a) 100% ZrO_2, (b) 85% ZrO_2 doped with 8% Y_2O_3 and (c) 85% ZrO_2 doped with15% Y_2O_3.

The phase diagram for the zirconia-yttria system is given in figure 9.The range of stability for each of these phases is shown below:

$$\text{Monoclinic} \underset{1173\,^oC}{\leftrightarrow} \text{Tetragonal} \underset{2370\,^oC}{\leftrightarrow} \text{Cubic}$$

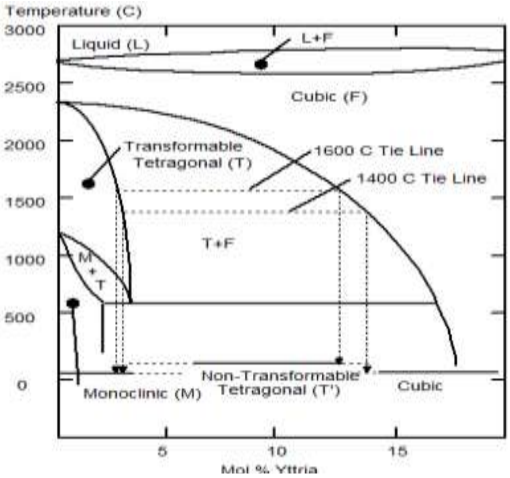

Figure 9: Phase Diagram for the Zirconia Yttria System.

The tetragonal to monoclinic transformation is of great technological significance, due to the martensitic nature of the reaction and the accompanying 3-5% volume expansion. The large volume and shape deformations, which occur through the martensitic transformation, set up large strains in the structure. These strains cannot be relieved by diffusion, instead they are accommodated by elastic or plastic deformation of the surrounding matrix. Martensitic reactions occur when the temperature is changing. The addition of yttrium oxide soluble in zirconia lowers the tetragonal to monoclinic (t-m) and cubic to tetragonal (c-t) transformation temperatures. The amount of alloying oxide required to produce stabilization is determined from the relevant phase diagram given in figure 9. Any composition which is fired in the cubic phase field and retains a wholly cubic structure on cooling is stated to be “fully stabilized” [19].

IV. Conclusions

In this research, the thermal expansion behavior of Al-based composites reinforced with zirconia nanoparticles without and with doping by yttria has been investigated. The results indicate that the experimental CTEs were within the Schapery’s bounds. The addition of yttrium oxide soluble in zirconia lowers the tetragonal to monoclinic (t-m) transformation.

References

[1] A. C. Reddy, Evaluation of mechanical behavior of Al-alloy/SiC metal matrix composites with respect to their constituents using Taguchi techniques, i-manager’s Journal of Mechanical Engineering, 1(2), 31-41, 2011.

[2] A. C. Reddy, Evaluation of mechanical behavior of Al-alloy/Al_2O_3 metal matrix composites with respect to their constituents using Taguchi, International Journal of Emerging Technologies and Applications in Engineering Technology and Sciences, 4(2), 26-30, 2011.

[3] A. C. Reddy, Tensile fracture behavior of 7072/SiCp metal matrix composites fabricated by gravity die casting process, Materials Technology: Advanced Performance Materials, 26(5), 257-262, 2011.

[4] A. C. Reddy, Combined Loading and Micromechanical Analysis of AA5050 Alloy-Silicon Oxide Particle-Reinforced Metal Matrix Composites, 5th International Conference on Modern Materials and Manufacturing, Bangalore, 6-7 December 2013, 373-378

[5] M. Mastanaih, A. C. Reddy, Exploitation of Reinforcement in Revision of Wear Behavior of AA1100/Si3N4 Metal Matrix Composites, 5th International Conference on Modern Materials and Manufacturing, Bangalore, 6-7 December 2013, 379-383

[6] V. K. Reddy, A. C. Reddy, Wear performance of AA4015/Boron Carbide Metal Matrix Composites, 5th International Conference on Modern Materials and Manufacturing, Bangalore, 6-7 December 2013, 384-388

[7] M. Mastanaih, A. C. Reddy, Influence of Reinforcing Particle Size on Tribological Properties of AA6061-Titanium Carbide Microcomposites, 5th International Conference on Modern Materials and Manufacturing, Bangalore, 6-7 December 2013, 389-393

[8] V. K. Reddy, A. C. Reddy, Role of Reinforcing Particle Size in the Wear Behavior of AA6061-Titanium Nitride Composites, 5th International Conference on Modern Materials and Manufacturing, Bangalore, 6-7 December 2013, 394-398

[9] V. B. Reddy, A. C. Reddy, Sliding Wear by Hard and Micro-Particles of AA2024-Zirconium Carbide Metal Matrix Composites, 5th International Conference on Modern Materials and Manufacturing, Bangalore, 6-7 December 2013, 399-403

[10] T. K. K. Reddy, A. C. Reddy, Wear Performance of Magnesia as Reinforcement of AA2024 Metal Matrix Composites, 5th International Conference on Modern Materials and Manufacturing, Bangalore, 6-7 December 2013, 404-408

[11] A. C. Reddy, Study of Factors Influencing Sliding Wear Behavior of Hexagonal Boron Nitride Reinforced AA6061 Metal Matrix Composites, 5th International Conference on Modern Materials and Manufacturing, Bangalore, 6-7 December 2013, 409-413.

[12] A. C. Reddy, Effect of Phase Transformation from h-BN to c-BN on Nanoparticle Fracture Tendency in AA8090/h-BN Particle-Reinforced Metal Matrix Composites, 5th International Conference on Modern Materials and Manufacturing, Bangalore, 6-7 December 2013, 365-372

[13] Taya, Minoru, R.J. Arsenault. Metal Matrix Composites; Thermo mechanical behaviour. Pergamon Press (1989).

[14] Platt, P.; Frankel, P.; Gass, M.; Howells, R.; Preuss, M. (November 2014). "Finite element analysis of the tetragonal to monoclinic phase transformation during oxidation of zirconium alloys". Journal of Nuclear Materials. 454 (1-3): 290–297.

[15] A. G. Evans, R. M. Cannon, Toughening of brittle solids by martensitic transformations, Acta Metallurgica, 34, 1986, 761.

[16] P.S. Turner, Thermal Expansion Stresses in Reinforced Plastics, Journal of Research of the National Bureau of Standards, 37, 239-250, 1946.

[17] E.H. Kerner, The elastic and thermo-elastic properties of composite media, Proceedings of the Physical Society, 69, 808–813, 1956.

[18] R. A. Schapery, Thermal expansion coefficients of composite materials based on energy Principles, Journal of Composite Materials, 2, 380-404, 1968.

[19] D. L. Porter, A. G. Evans, A. H. Heuer, Transformation toughening in PSZ,. Acta Metallurgica, 27, 1979, 1649.